



ISSN-1232-5317

PL0001652



INSTYTUT ENERGII ATOMOWEJ
INSTITUTE OF ATOMIC ENERGY

RAPORT IAE - 46/A

**ANALYSIS OF UO₂ FUEL STRUCTURE
FOR LOW AND HIGH BURN-UP AND ITS IMPACT
ON FISSION GAS RELEASE**

MARCIN SZUTA¹
MOUSTAFA S. EL-KOLIEL²

¹Institute of Atomic Energy, 05-400 Otwock-Świerk, Poland

²Atomic Energy Authority, Reactors Department, 13759 Cairo, Egypt

**INSTYTUT ENERGII ATOMOWEJ
INSTITUTE OF ATOMIC ENERGY**

RAPORT IAE - 46/A

**ANALYSIS OF UO₂ FUEL STRUCTURE
FOR LOW AND HIGH BURN-UP AND ITS IMPACT
ON FISSION GAS RELEASE**

MARCIN SZUTA¹
MOUSTAFA S. EI-KOLIEL²

¹Institute of Atomic Energy, 05-400 Otwock-Świerk, Poland

²Atomic Energy Authority, Reactors Department, 13759 Cairo, Egypt

OTWOCK - ŚWIERK 1999

Marcin Szuta, Moustafa S.El-Koliel: Analysis of UO₂ Fuel Structure for Low and High Burn-up and Its Impact on Fission Gas Release. During irradiation, uranium dioxide (UO₂) fuel undergo important restructuring mainly represented by densification and swelling, void migration, equiaxed grain growth, grain subdivision, and the formation of columnar grains. The purpose of this study is to obtain a comprehensive picture of the phenomenon of equiaxed grain growth in UO₂ ceramic material. The change of grain size in high-density uranium dioxide as a function of temperature, initial grain size, time, and burnup is calculated. Algorithm of fission gas release from the UO₂ fuel during high temperature irradiation at high burnup taking into account grain growth effect is presented. Theoretical results are compared with the experimental data.

Marcin Szuta, Moustafa S.El-Koliel: Analiza struktury paliwa UO₂ niskich i wysokich wypaleń i jej wpływ na wydzielanie gazowych produktów rozszczepienia. Podczas napromieniania neutronami struktura paliwa UO₂ podlega znacznym zmianom, takim jak densyfikacja i puchnięcie, migracja wakansji, równomierny wzrost ziaren i podział ziaren oraz tworzenie ziaren słupkowych. Celem pracy jest uzyskanie pełnego opisu zjawisk równomiernego wzrostu ziaren w materiale ceramicznym UO₂. Przedstawiona jest zmiana wielkości ziaren w funkcji temperatury, początkowej wielkości ziaren i wypalenia. Przedstawiono algorytmy wydzielania gazowych produktów rozszczepienia z paliwa UO₂ podczas napromieniania w wysokich temperaturach dla wysokich wypaleń. Dokonano porównania rezultatów analiz teoretycznych z danymi eksperymentalnymi.

1. INTRODUCTION

A common fuel-element design consists of solid, high density, sintered cylindrical pellets of UO_2 inside a metal can. During irradiation the central temperature is often high enough to result in marked microstructural changes in the UO_2 fuel. A typical cross-section through an irradiated fuel can be divided radially into three structural regions. These are an unrestricted outer zone with as fabricated fuel grains, an inner annulus exhibiting equiaxed grain growth that contains enlarged fuel grains with all sides approximately the same length, and a central region of columnar grains [1]. Typically there is an axial void at the center of the pellet and an outer shell of small grains of 100 to 300 nm diameter and a high porosity of up to 30% with a typical thickness of 100 to 200 μm (rim structure)[2]. The structural regions of irradiated fuel, such as a columnar grain zone and a central void are observed only in fuels experiencing high powers and high temperature during irradiation [3], whilst, the rim structural (grain subdivision) is observed only in the high burnup fuel, where the local burnup threshold for the formation of rim structure was estimated to be about 60 or 70 – 80 GWd/tU . [4]

At fuel temperatures $T < 1000\text{ }^\circ\text{C}$ the grain size is identical to that of comparable un-irradiated material. No grain growth occurs below this particular temperature. At higher temperatures the grain size increases approximately exponentially, consistent with a-thermally activated process. It is known that significant equiaxed grain growth in Light Water Reactor (LWR) fuels occurs at temperatures above $\sim 1500\text{ }^\circ\text{C}$ [3]. It is also known that columnar grain growth can occur by a sublimation process at high temperatures ($>1700\text{ }^\circ\text{C}$) with a steep radial gradient (for example, $2000\text{ }^\circ\text{C/cm}$). Linear power in excess of $\sim 60\text{ kW/m}$ is required to achieve the temperatures and temperature gradients necessary for columnar growth. Columnar grain growth is not expected to occur in LWR fuels even under transient conditions. Although the fuel temperature and radial temperature gradients may exceed the threshold values for columnar growth, this transient condition usually exists for only a short period. [4-6]

Fuel temperature is the most essential input in the evaluation of grain growth. In addition to time and temperature variables, grain growth behavior dependent on factors such as stoichiometry, impurities and porosity. [5]

In practice, one distinguishes between “normal” or “continuous” grain growth and “abnormal” or “discontinuous” grain growth. [7] During normal grain growth, the size of the individual grains are relatively uniform. During abnormal grain growth, on the other hand, the

differences in individual sizes increase by some of the grains growing rapidly. When they have consumed all the other grains, the remaining grains may again be of a relatively uniform size.

Grain size is one of the most important parameters that affect fission gas release or retention during fuel irradiation. The UO_2 fuel of large grain size is recognised as desirable since it can reduce the amount of fission gas released during irradiation. The major contributions to fission gas release from irradiated UO_2 fuel to the fuel exterior arise when (i) intergranular bubbles coalesce to form interconnectivity tunnels, or (ii) when cracks due to power transients intersect the bubbles-weakened boundaries. This is because that, initially, the fission gas produced in the fuel lattice during irradiation reaches the grain boundaries by diffusion from the grains, and by collection of gas by grain growth mechanism, where they form gas bubbles on the grain boundary surfaces.[8]

2. EXPERIMENTAL OBSERVATIONS

There are several experimental observations [9-13] that assist the model development, and confirm our assumptions, these information could be summarised as follows:

1. It has been known for over a century that in the presence of an electric discharge or electron beam, gas atoms become embedded into the electrodes and the walls of the vessel containing the gas. It is proved also that irradiating the UO_2 pellets in the presence of natural xenon, part of the gas is embedded into the pellet. Whilst the gases embedded by electric discharge are only lightly attached to solid surfaces and can easily be released by slight heating, the xenon is found to be firmly attached to the UO_2 surface such that only 1% of the attached gas can be removed after annealing samples for over 12 hours at 1400 °C. [9,10]
2. The samples of uranium oxides with different U/O ratios ranging from 2.00 to 2.62, irradiated to a total fission fluency 10^{15} fissions/cm³ revealed during annealing three main peaks of xenon release [11]. For instance, for the $\text{UO}_{2.14}$ sample the three peaks lie in the temperature ranges 180 - 250 °C, 600 – 650 °C and about 1000 °C. The first peak in the range 180 – 250 °C can be the result of gas migration from under surface flaws and voids what is proved by low activation energy (about 10 kcal/mole) and relatively small amount

of released gas (5 – 7 %). Thermal recovery of irradiation defects and microstructure change in irradiated UO_2 fuels studied by X – ray diffraction and transmission electron microscopy explain that the gas release kinetics from irradiated UO_2 is determined by the kinetics of thermal recovery of the irradiation induced defects.

3. The point defects induced by irradiation begin to recover around at 450 – 650 °C and almost completely are recovered above 850 °C, while defect clusters of dislocation and small intragranular bubbles are recovered in the range 1150 – 1450 °C.[12]
4. Out of pile experiments show that annealing the irradiated UO_2 samples, bursts of fission gas release occur [13]. After a small burst release at relatively low temperatures, a large burst release appears at high temperature. The critical temperature of high temperature burst release is about 1800 °C for low burn-up (about 7 MWd/kgU) and decreases to about 1500 °C for high burn-up (30 MWd/ kgU).
5. The process of grain sub-division at high burn-up of (70 – 80 MWd/kgU) forms an extremely fine structure to a temperature as high as 1100 °C, and decrease of fission gas concentration in the fuel lattice is observed [16]. Also the re-crystallized grain region is found to be adjacent to the sub-divided grain region and in the re-crystallized grain no defects or bubbles are observed. [17]

3. ANALYSIS AND ASSUMPTIONS

In our opinion the low burn-up burst release is a medium value of the three peaks of fission gas release mentioned above [13] which could be distinguished if the heating rate (100 °C/min) was significantly lower. If the point defects, defect clusters of dislocations and small intragranular bubbles are thermally recovered at high temperature of fission gas burst, then what strength are to immobilise the noble gases. Hence an additional trapping process of inert gas atoms with the uranium dioxide material is to occur.

The process of strong binding of the fission gas fragments with the irradiation defects is described in the open literature as a process of chemical interaction with the UO_2 [14]. It is assumed that the vicinity of the fission fragment trajectory is the place of intensive irradiation induced chemical interaction of the fission gas products with the UO_2 .

The fission fragments which are heavily charged ions with initial energy approximately 100 MeV interact strongly with electrons of the material losing their energy mainly by ionisation and also by elastic collisions with atoms as a whole. The fission fragments are striped of about 20 electrons along most of their paths in the medium in which the fission takes place. The charge of the fission fragments is still 10 at the end of their path [15]. When fission fragments have dissipated all their energy, they stop in the material and called fission products.

The fission fragment causes intense ionisation along its track and creates what might be called an “electron spike”. In a metal or a good conductor this is dissipated very quickly via the free electron system and electrical neutrality is soon restored. On the other hand, in an insulator or poor conductor, there are no free electrons and the electron spike is relatively slow to dissipate, with the result that the region of net positive charge which is created along the track can persist for rather long times relative to that expected in a metal.

We assume that the area of atomic disorder remaining after the passage of a fission fragment can bind charged fission gas fragments and prevent their mobility. The process of strong binding of the fission gas fragments with the irradiation defect can occur only during fissioning.

The highly charged fragments of Kr and Xe at the end of their paths can also become neutral by attracting the needed electrons and become single gas atoms. When the fission gas products are not charged then they behave according to the rules of classical diffusion. It can be assumed that above a limiting value of fission fluency (burn-up) occurs a more intensive process of irradiation induced chemical interaction until the diffusion of single gas atoms is insignificant. Hence significant part of fission gas product is expected to be chemically bound in the matrix of UO_2 .

Furthermore it is expected that the gas can be released in the process of re-crystallization. The higher fission fluency (burn-up) the higher amount of gas should be released and the lower re-crystallization temperature should be observed.

The critical temperature decrease with fission fluency (burn-up) suggests that the re-crystallization temperature of UO_2 is changed by the process of chemical interaction. Consequently, during irradiation the grain growth should be observed above the re-crystallization temperature and division of grains should be observed below the temperature when saturation is obtained. This means further that the re-crystallized region will be adjacent

to the subdivided grain region and the division surface of the two regions will be assigned by the re-crystallization temperature. It can also be expected that in the re-crystallized grains the defects are swept out.

This seems to be natural since the chemically bound fission gas atoms replacing for instance uranium atom in the crystallographic lattice can form weak facets what should decrease re-crystallization temperature the more fission gas atoms are retained and where division of the grains can occur when saturation is obtained and simultaneously the increase of fission gas products release is to be expected.

The decrease of critical temperature for fractional fission gas release from the fuel above 1 % to a value about 1100 °C for high burn-up reported by Vitanza et al. [18] well correlates with the experiments [13] and [16] mentioned above. This also gives evidence for the concept of chemical interaction of the fission gas atoms with the atoms of fuel. We assume further that all the retained gas atoms in the lattice are released from the grain volume which re-crystallized. Assuming that the Vitanza curve [18] describes the change of uranium dioxide re-crystallization temperature, we can say that the modification of grain growth rate correlation is to be dependent on burn-up so to obtain the best fit of the grain size change with the curve.

4. THEORETICAL MODELS FOR EQUAXED GRAIN GROWTH

Examination of micrographs of UO₂ during normal grain growth makes it clear that the pores remain on grain boundaries, and more commonly at grain intersections. This means that, in contrast to solid inclusions, which remain relatively stationary and permit only local boundary movement or complete boundary breakaway, the pores must migrate along with the boundaries during normal grain growth. [7]

In ceramics such as UO₂, where gas bubbles are situated on grain boundaries, the dragging of bubbles by grain boundaries has been proposed as one of the possible driving forces for the migration. These bubbles impede the growth of grains, this resistance increasing with both the bubble size and their concentration on grain boundaries. Eventually, when the driving force for grain growth equals the drag from bubbles, no further grain growth will occur. An analysis, due to Zener,[19] suggests that, in a solid containing a stable array of inclusions and/or pores, grain growth will cease at some limiting grain size, D_m , given by

$$D_m = \frac{8}{3 \sum f_i / r_i} \quad (1)$$

Where f_i is the volume fraction of pores or inclusions with radius r_i . Speight and Greenwood [8] performed an analysis that shows bubbles could not prevent the movement of grain boundaries, but their effect was to reduce the velocity of movement. The small bubbles move rapidly and remain attached to the grain boundaries, whereas large bubbles or pores move slowly and have the greatest effect in retarding the movement of the grain boundaries before a complete break-away occurs, or left behind the boundaries. R.D. MacDonald [20] has observed this effect during the post-irradiation examination of an arc-cast uranium carbide (4.7 wt% C) specimen.

Speight and Greenwood [8] derived an expression for the grain boundary velocity, V , when the boundary's surface, with radius of curvature R , is decorated by N gas bubbles per unit grain boundary area, each of radius r . Their result can be written as:

$$V = C \left(\frac{1}{R} \right) [1 - F(R, N, r, \phi)] \quad (2)$$

Where C is a temperature-dependent constant and F is the retarding function to boundary motion due to the attached gas bubbles. It is an expression of the geometrical parameters R , r , N and $\sin 2\phi$ where ϕ is the drag angle between bubbles and boundary. The boundary velocity is also the rate of growth of the average diameter grain (dD/dt), so that Eq. 2 is also the grain growth law for the UO_2 fuel.

Several models [21-29] for grain growth have been developed to predict grain growth in UO_2 as a function of time and temperature. These different models correspond to different mass transport mechanisms.

The driving force for equiaxed grain growth is the decrease in surface free energy brought about by the decrease in the number of grains, and, consequently, a decrease in the total surface grain boundary surface area. The grain boundaries move outward from the center of curvature, and generally, the net result of grain boundary movement is shrinkage of small grains with predominately convex surfaces, where, large grains consume small ones. The growth is at a rate proportional to the curvature or inversely proportional to the grain diameter giving a growth law of the form: [5,21]

$$\frac{dD}{dt} = \frac{k}{D} \quad (3)$$

on integration we find;

$$D^2 - D_0^2 = 2kt = k_0 t \exp\left(-\frac{Q}{RT}\right) \quad (4)$$

Where k is a proportional constant, D and D_0 are instantaneous and initial grain size, respectively, t is time, Q is activation energy (J/mol), R is gas constant (1.986 cal/K.mol), and T is absolute temperature. Another empirical models describing grain growth kinetics are in literature [22-25]. A cubic grain growth equation is obtained by assuming a vapor transport mechanism with pore pressure in equilibrium with UO_2 surface tension [22]:

$$D^3 = D_0^3 + k_0 t \exp\left(-\frac{Q}{RT}\right) \quad (5)$$

A fourth-order grain growth equation is obtained assuming vapor transport with constant pore pressure:[23]

$$D^4 = D_0^4 + k_0 t \exp\left(-\frac{Q}{RT}\right) \quad (6)$$

Other authors [24] recommended the following kinetic equations:

$$D^{2.5} = D_0^{2.5} + k_0 t \exp\left(-\frac{Q}{RT}\right) \quad (7)$$

Grain growth is conveniently described by the following general form: [25]

$$D^n - D_0^n = k_0 t \exp\left(-\frac{Q}{RT}\right) \quad (8)$$

MacEwan and Hayachi [26] originally obtained a best fit to data from the range 1830 to 2710 K with $n = 2.5$. Singh [27] reported data from 2100 - 2400 K which fitted a cubic rate law, where no columnar grain growth was observed. Hsieh [23] suggested that the fourth-order grain growth kinetics is more suitable for modeling purposes of LWR fuels. In fact, for sintered oxide materials the value of n is very difficult to determine because of the influence exercised by the porosity, impurities and by the OM ratio of the investigated materials. These parameters can retard or accelerate the movements of the grain boundaries in different ways

especially at low temperature. In general, in the above expressions, the value of the exponent n ranges from 2 to 5, Q from 240 to 620 KJ/mol., and k_0 from 4×10^6 to 7×10^{15} . [28]

5. MODIFICATION OF GRAIN GROWTH EQUATION

It is known that the porosity which exists in the fuel before the irradiation plus the gaseous and solid fission products are effective in retarding the rate of grain growth (see section 4). All the above models don't take under consideration this retardation effect. Another model assumes that grain growth continuous until some limiting grain size has been reached. Ainscough et al. [29] performed measurements of equiaxed grain growth at temperatures between 1300 to 1500 °C over fairly long periods (up to 24 weeks). Ainscough et al. [29] correlated these data using Burke's [21] concept, which takes account of the retarding forces arising from interactions with inclusions or with pores. The magnitude of this additional force per area of boundary is a constant independent of grain size. Burke [21] has proposed the following expression for the rate of change of the grain size with respect to time:

$$\frac{dD}{dt} = k \left(\frac{1}{D} - \frac{1}{D_m} \right) \quad (9)$$

with

$$k = 5.24 \times 10^7 \exp \left(- \frac{2.67 \times 10^5}{RT} \right) \quad (9a)$$

and

$$D_m = 2.23 \times 10^3 \exp \left(- \frac{7620}{T} \right) \quad (9b)$$

where

- D - grain diameter (μm),
- D_m - limiting grain size (μm) at which grain growth ceases,
- R - the gas constant equal 8.314 J/mol/K,
- k - grain growth rate constant ($\mu\text{m}^2/\text{h}$),
- T - Temperature (K),
- t - time (h)

It was found that the concentration of fission products is effective in retarding grain growth (see section 4). Ainscough modified Eq. 9. to allow for the increasing retarding effect of fission products by writing:

$$\frac{dD}{dt} = k \left(\frac{1}{D} - \frac{f(Bu)}{D_m} \right) \quad (10)$$

The grain growth model of Ainscough et al. [29] is generally considered to be the best available one. To solve Eq. 10. it is necessary to know the initial grain size. Where $f(Bu)$ representing the fractional reduction in the maximum grain radius by irradiation, is given by

$$f(Bu) = (1 + 0.002 \times Bu) \quad (11)$$

Where **Bu** is the burn-up in MWd/tU. Applying Eq. 11 to the calculations of grain size, a smaller value of the limiting grain size can be expected. So, the limiting grain size, D'_m , dependent on temperature and burn-up will be equal:

$$D'_m = \frac{D_m}{1 + 0.002 \times Bu} \quad (12)$$

On integration, Eq. 9. Gives:

$$D_m(D_0 - D) + D_m^2 \ln \left(\frac{D_m - D_0}{D_m - D} \right) = kt \quad (13)$$

But Eq. 10 can no longer be integrated analytically.

Comparing the empirical data of limiting grain size influenced by irradiation conditions presented in the work [30] with the limiting grain size described by Eq. 11 we came to the conclusion that the function $f(B)$ dependent on burn-up is:

$$f(Bu) = 1 + 0.00002 \times Bu \quad (14)$$

The coefficient k in the simple rate Eq. 9 describes the term of grain growth rate dependent on temperature. However, the out-of-pile annealing experiments referring to the burst of fission gas release [13], the decrease of critical temperature for fractional fission gas release from the fuel above 1 % [18] and the in-reactor experiments of grain growth in function of temperature [29] for different burnups imply that the coefficient k should also depend on burnup. Eq. 9a

presents the coefficient k for the un-irradiated UO_2 fuel. So, the temperature in Eq. 9a should be increased by the value dependent on burnup, thus to obtain the Vitanza curve. It means that the re-crystallization temperature occurs at earlier temperatures when the burnup is higher. The increase of temperature depending on burnup Bu can be described by the following equation:

$$\Delta T = \Delta T_0 \left(1 - e^{-\frac{Bu}{B_0}} \right) + AB \quad (15)$$

On the basis of the fact that the re-crystallization temperature for un-irradiated UO_2 occurs at about 1670 °C, and the indirect evidences of the experimental data [16,18], show that the re-crystallization temperature for highly irradiated UO_2 is equal 1150 °C, the constant ΔT_0 is estimated to be about 500 °C.

The constants B_0 and A are estimated from Vitanza curve [18]:

$$B_0 \approx 2700 \text{ MWd/tu}$$

$$A \approx 0.014$$

Finally, the grain growth constant k in the simple rate equation obtains the form:

$$k = 5.27 \times 10^7 \exp \left(- \frac{2.67 \times 10^5}{R(T + 371 \times (1 - \exp(-\frac{Bu}{2700})) + 0.014 \times Bu)} \right) \quad (16)$$

The above considerations show that the irradiation damage (burnup) introduced by fission events have two opposing effects on grain growth. The large concentration of fission gas atoms in the lattice introduced in fission spikes enhances the transfer of atoms across a boundary, increasing the rate of growth. The higher is burnup, the higher is the value of k and consequently the higher is the grain growth rate. Conversely, the impurities (burnup) introduced by fission inhibits growth. The higher is burnup the lower is the limiting grain size (see Eq. 12).

If we put the modified retardation effect function defined by Eq. 14 and the grain growth constant rate defined by Eq. 16 into Eq. 10, and solving it numerically using fourth order Runge-Kutta integration method, we have obtained a reasonable agreement with the experimental data of in-reactor grain growth versus temperature for two different burnups –

see Figs. (1 and 2). Fig. (1) shows data measured during post irradiation examination, as a function of temperature at fuel burnup of 6560 MWd/tU. The solid line represents the calculated grain size as a function of temperature. The re-crystallization of UO_2 at this burnup occurs at about 1300°C . The initial grain size of $5.6 \mu\text{m}$ is used in the calculations. Also, Fig. (2) compares our results with the measured data at 12865 MWd/tU, where the recrystallization starts earlier than the previous one. This is due to in fact, the increased burnup. The UO_2 fuel starts to recrystallize at about 1200°C . The initial grain size of $4.7 \mu\text{m}$ is used in the calculations. 10 % of grain size increase for burnup of 6560 MWd/tU occurs at about 1300°C (Fig. 1) and for burnup of 12865 MWd/tU at about 1200°C (Fig. 2). This correlates very well with the Vitanza curve, and confirms our assumption that Vitanza curve represents the recrystallization temperature.

Vitanza et al. [18] correlated a relation between the central fuel temperature and the burnup for fission gas release by fitting to experimental data. Vitanza curve is based on in-core data of internal rod pressure and fuel center temperature until the occurrence of 1% fission gas release, where these data are obtained from instrumented fuel rods. In this study we have modified the grain growth rate to be dependent on burnup so to obtain the best fit of the grain size change with temperature burnup dependent. So, we can obtain a curve showing relation between the recrystallization temperature and fuel burnup. Below this curve insignificant fission gas release will occur. The results obtained from our model are compared in Fig. (3) together with the Vitanza curve. Fitting the curve of re-crystallization temperature in function of burnup with the Vitanza curve is fairly good but for low burnup. As Vitanza curve describes the critical temperature of fractional fission gas release from fuel above 1% in function of burnup [18], and for low burnup the single gas atom diffusion is most significant in fission gas release [31], it means the process of re-crystallization for low burnup is negligible. So the comparison of Vitanza curve with the re-crystallization temperature versus burnup has no basis for low burnup.

The same above principle of temperature appointment at 10 % grain size increase allows us to invent the curve of re-crystallization temperature versus burnup (Fig. 3) from the family curves of grain growth in function of temperature for different burnups (fig. 4). The variation in grain size versus temperature for different values of burnups is shown in fig. (4). At fuel temperatures $T < 1300 \text{ K}$ the grain size is $\sim 6 \mu\text{m}$; identical to the input size, since there is no

grain growth below this particular temperature. At higher temperatures the grain size increases approximately exponentially, consistent with a thermally activated process.

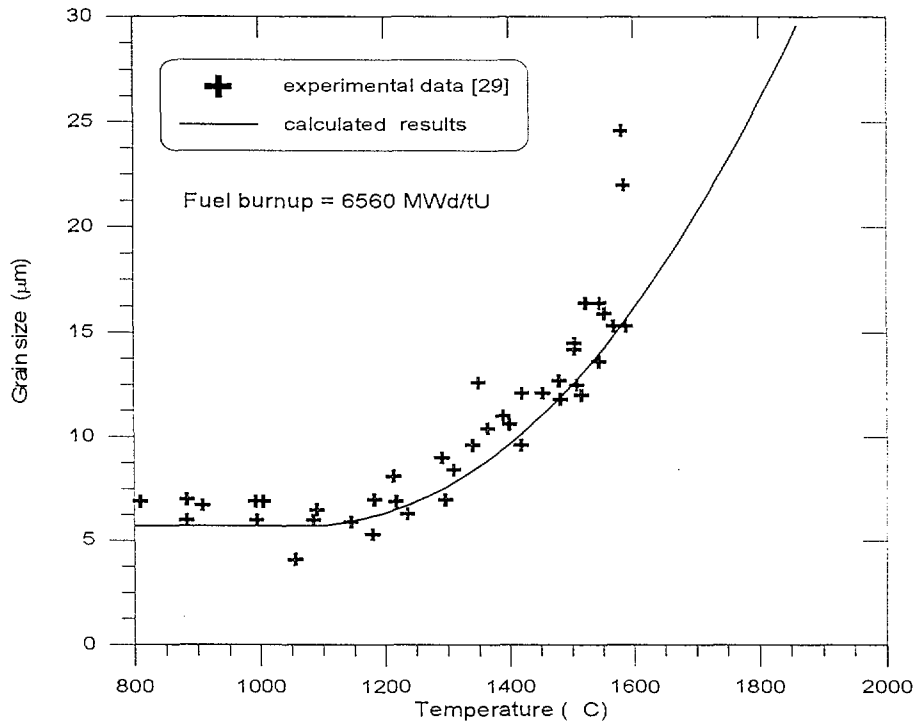


Fig. 1. Comparison of measured and calculated fuel grain growth results.

As the temperature increased the grain diameter attained a maximum of ~ 14, 26, 43, and 63 μm at 1300, 1500, 1700 and 1900 $^{\circ}\text{C}$, respectively, although, the time of annealing is the same for all these temperatures. The grain size for non-irradiated UO_2 doesn't change up to the temperature 1600 $^{\circ}\text{C}$, while for high burnup of 50 000 MWd/tU doesn't change up to 1100 $^{\circ}\text{C}$. We can notice that the higher burnup, the lower re-crystallization temperature. The burnup is considered as the parameter which governed the retarding effects on grain growth. Fig. 5 clearly demonstrates the change of grain size as a function of time for constant temperature of 1300 $^{\circ}\text{C}$ and, for different values of fuel burnup, where two opposing effects of enhancement and inhibition of irradiation damage introduced by fission effect on equiaxed grain growth rate are described. Also, the change of grain size as a function of time for constant burnup of 6560 MWd/tU and for different values of temperatures is shown in fig. 6. Grain sizes of ~ 62, 42, 26

and 13 μm is expected at 1900, 1700, 1500 and 1300 $^{\circ}\text{C}$ respectively. The above results show the change of grain size in function of fuel temperature and burnup.

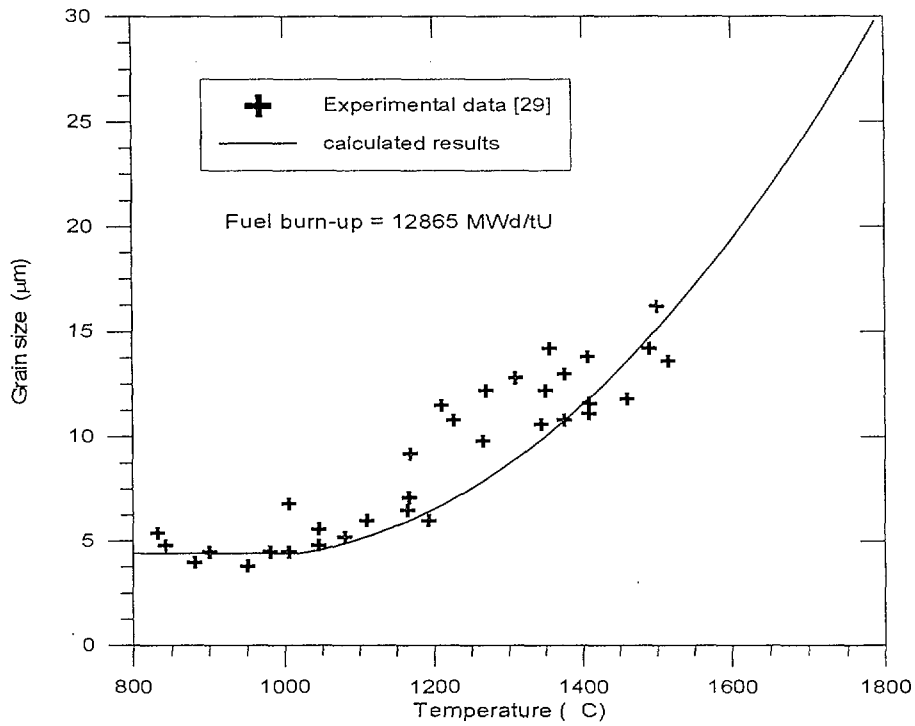


Fig. 2. Comparison of measured and calculated fuel grain growth results

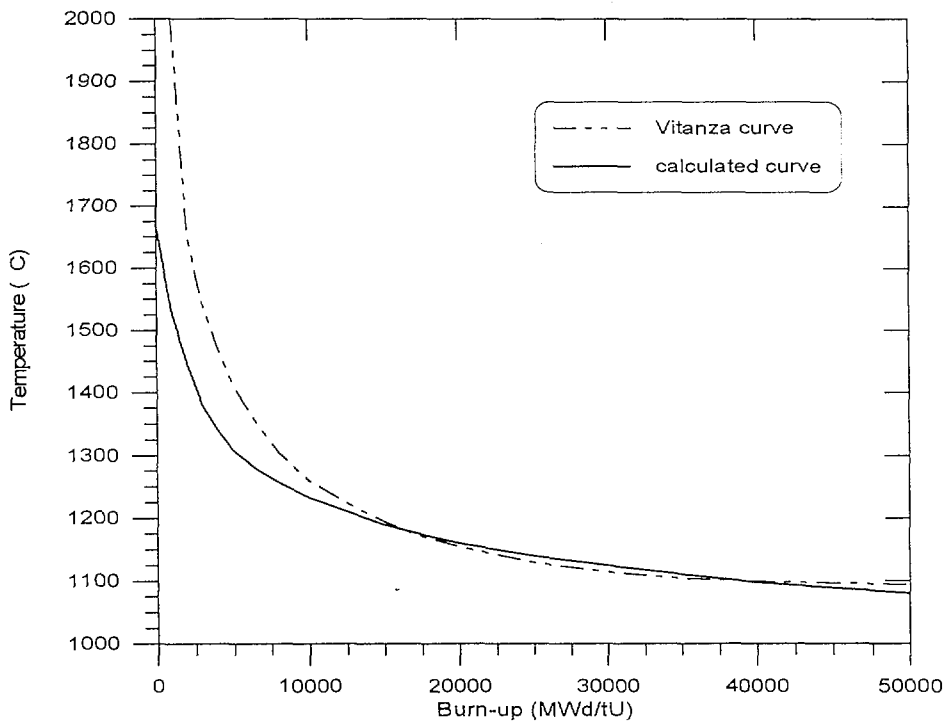


Fig. 3. Comparison between the calculated recrystallization temperature and Vitanza curve [19].

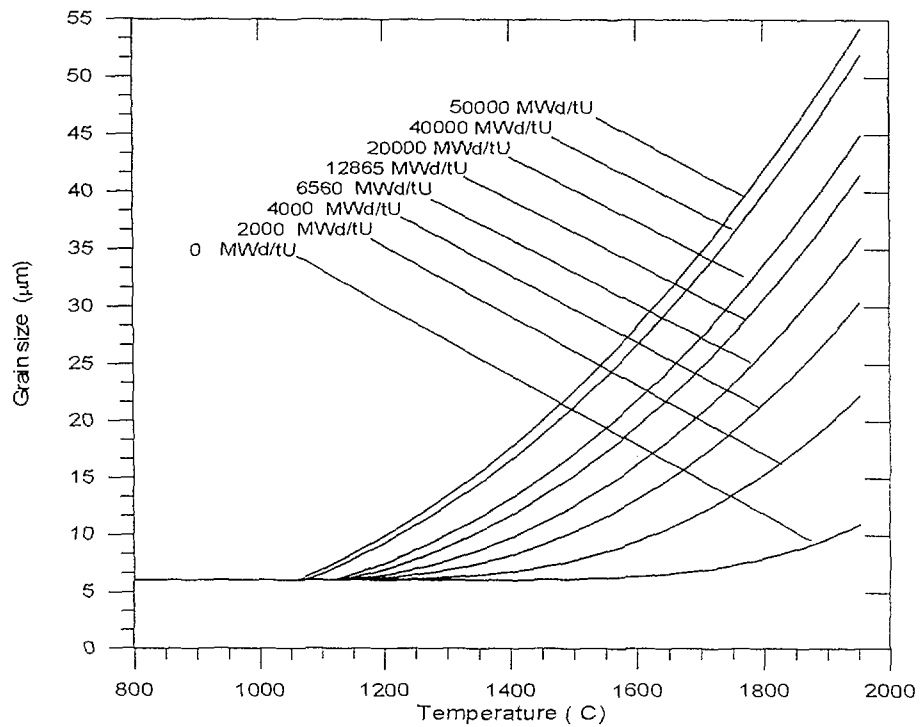


Fig. 4. Fuel grain growth as of fuel temperature for various values of fuel burn-up

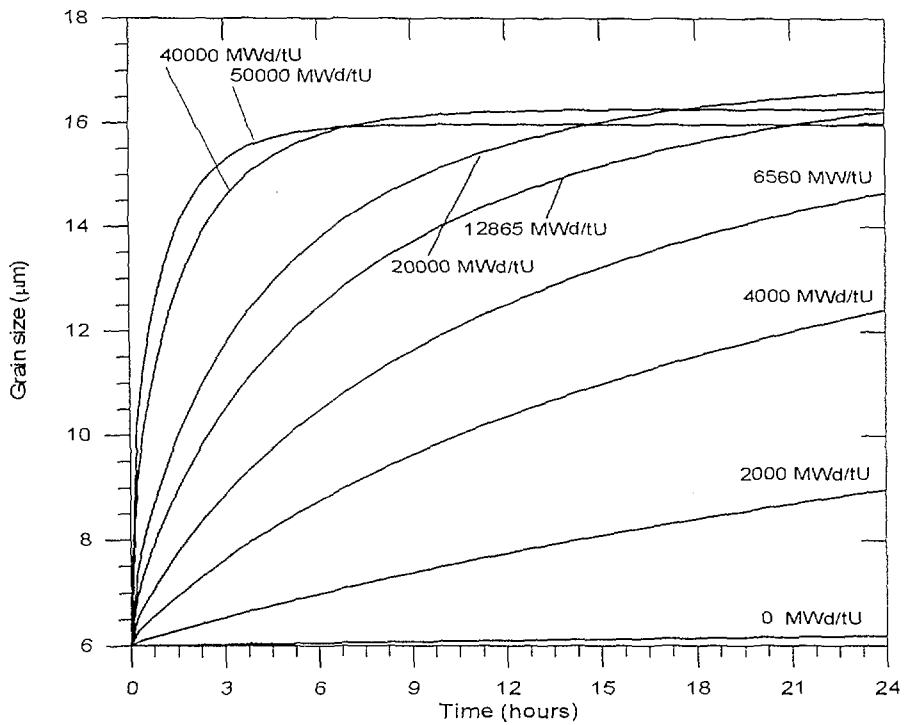


Fig. 5. Grain growth as a function of time for several values of fuel burnups and at the constant temperature of 1300 C.

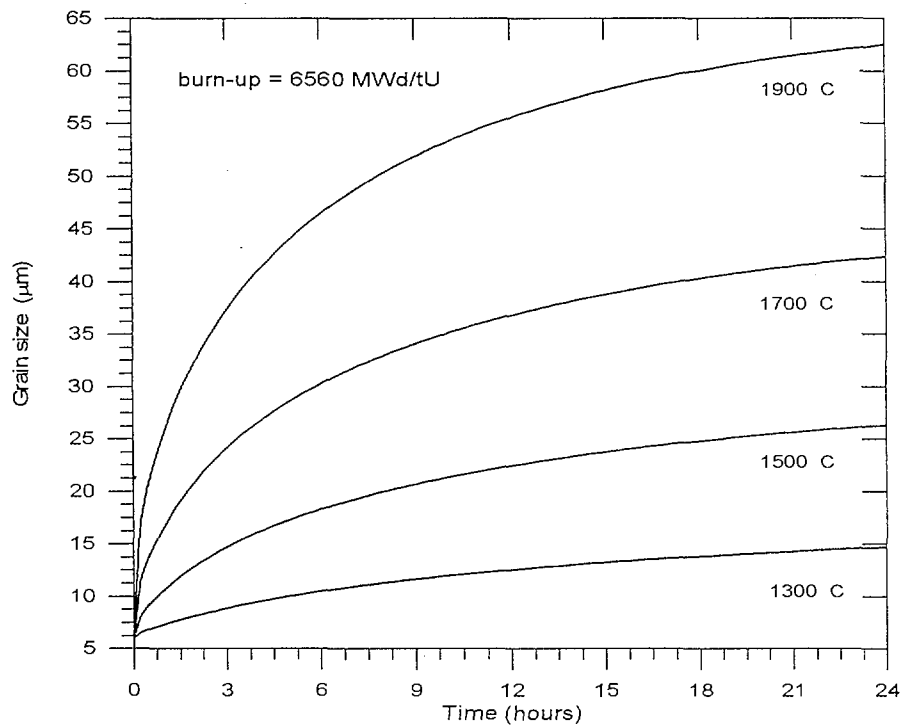


Fig. 6. Grain growth as a function of time for different values of fuel temperature

6. ALGORITHMS OF FISSION GAS RELEASE DUE TO RECRYSTALLIZATION OF UO_2 GRAINS

It is generally accepted that most of the insoluble inert gas atoms of xenon and krypton produced during fissioning are retained in the fuel irradiated at temperature lower than the threshold [31–39]. We assume that most of the gas atoms are retained in the matrix of grains being there immobilised or are precipitated into small fission gas bubbles. We assume further that the retained gas atoms in the fuel are released from the grain volume which re-crystallized.

The defect trap model of fission gas behaviour in UO_2 fuel described in the papers [31, 40, 41, and 42] is to be completed of the grain growth process. In the model it is assumed that the fission gas atoms trapped in the matrix of UO_2 and that trapped in bubbles exist side by side with the intermediate gas, which consists of the gaseous fission fragments and the kinetically excited fission gas products. The processes of re-solution, knock-out and bubble diffusion are modelled.

It is well established that grain growth in polycrystalline materials is caused by the preferential shrinkage of smaller grains due to their comparative smaller radii of curvature. An average number of grains, (N_0), in unit volume is:

$$N_0 = \frac{1 - \frac{p}{100}}{\frac{4}{3}\pi\left(\frac{D_0}{2}\right)^3} \quad (17)$$

where

p – porosity in %,
 D_0 – initial grain diameter.

The number of grains, (N), in unit volume at the elevated temperature is fixed by the limiting grain size, D_m :

$$N = \frac{1 - \frac{p}{100}}{\frac{4}{3}\pi\left(\frac{D_0}{2}\right)^3} \quad (18)$$

The initial grain size, D_0 , is easily measurable while the limiting grain size, D_m , is determined from Eq. 12. The released fraction of fission gas atoms for stable state, f_r , due to recrystallization is calculated as follows:

$$f_r = \frac{N_0 \frac{4}{3}\pi\left(\frac{D_0}{2}\right)^3 - N \frac{4}{3}\pi\left(\frac{D_0}{2}\right)^3}{N_0 \frac{4}{3}\pi\left(\frac{D_0}{2}\right)^3} = 1 - \left(\frac{D_0}{D_m}\right)^3 \quad (19)$$

The Eq. 19. shows that the initial grain size strongly affects the fission gas release and reduces the fission gas release with increasing it. This conclusion is supported by the experimental results [34].

In order to complete the set of differential equations of the defect trap model of fission gas behaviour the release rate of re-soluted gas and trapped in the bubbles is to be determined. Multiplying the rate of change of grain volume by the concentration of re-soluted gas atoms in

the matrix, M_r , and trapped gas atoms in the bubbles, M_{tr} , we obtain the release from one grain, R_{go} due to grain growth process:

$$R_{go} = \frac{1}{2} \pi (M_r + M_{tr}) D^2 \frac{dD}{dt} \quad (20)$$

Where dD/dt is determined from Eq. 10 and Eqs. (14 and 16). The product of release rate from one grain, R_{go} , and the number of grains, N , at elevated temperature defined by Eq. 18 determines the release rate from unit volume. Finally, the mathematical model presented previously is supplemented with fission gas release due to grain re-crystallization according to the above-presented assumptions:

$$\frac{dN_{tr}^{ko}}{dt} = g_1 f - (g_2 + g_3) f N_{tr}^{ko} \quad \text{for } 0 \leq x \leq r \quad (21)$$

$$\frac{\partial N_{tr}^D}{\partial t} = D_b \nabla^2 N_{tr}^D - (g_2 + g_3) f N_{tr}^D \quad \text{for } 0 \leq x \leq r \quad (22)$$

$$\frac{\partial N_{trII}^D}{\partial t} = D_b \nabla^2 N_{trII}^D + g_1 f - g_3 f N_{trII}^D \quad \text{for } 0 \leq x \leq \infty \quad (23)$$

$$\frac{dM}{dt} = \beta_i f + \alpha_1 f M_r + g_3 f M_{tr} - \alpha_2 M - g N_{tr} M \quad (24)$$

$$\frac{dM_{tr}}{dt} = g N_{tr} M - g_2 f M_{tr} - g_3 f M_{tr} - \lambda M_{tr} - \frac{1}{2} \pi M_{tr} D^2 \frac{dD}{dt} N \quad (25)$$

$$\frac{dM_r}{dt} = \alpha_2 M - \alpha_1 f M_r - \lambda M_r - \frac{1}{2} \pi M_r D^2 \frac{dD}{dt} N \quad (26)$$

$$R = g_2 f M_{tr} (S \times r) + \frac{1}{2} \pi (M_{tr} + M_r) D^2 \frac{dD}{dt} N \quad (27)$$

Where

$$\langle N_{tr}^D \rangle = \frac{1}{r} \int_0^r N_{tr}^D dx \quad (28)$$

$$N_{tr} = N_{tr}^{ko} + \langle N_{tr}^D \rangle \quad (29)$$

$$S = S_0 + S_1 \left(1 - \exp \left(- \frac{Bu - B_0}{\tau} \right) \right) \quad (30)$$

- N_s - concentration of bubbles in the surface layer,
 λ - decay constant of isotope i ,
 β_i - formation yield of the intermediate gas of isotope i ,
 f - fission rate,
 t - time,
 x - distance into the fuel from the sample surface,
 r - fission product range,
 D_b - diffusion coefficient of bubbles,
 Bu - burnup,
 M - concentration of intermediate gas atoms,
 M_{tr} - concentration of gas atoms in the bubbles,
 M_r - concentration of gas atoms in the matrix,
 S - total surface area,
 $g, g_1, g_2, g_3, \alpha_1, \alpha_2, S_0, S_1, B_0, \tau$ - constants.

It is assumed that the total surface area versus burnup described by Eq. 30 does not change during the process of grain growth. The coupled Eqs. (21-30) are solved numerically using the modified Runge-Kutta method and the explicit finite-difference technique; Crank-Nicholson scheme.

7. COMPARISON WITH EXPERIMENTS

When grain growth occurs, the gases are released more rapidly than they are released by knock-out process. Two cases of calculations were conducted to examine the influence of grain growth on fission gas release. One case was calculated, for the temperature 1100 °C, including grain growth, and the other, for the temperature 1000 °C, it means no grain growth occurred. The initial grain size of 8 μm. and the fission rate $f = 10^{14}$ fissions/cm³/s were used in the calculations. Fig. (7) provides the results of two cases compared with the experimental

data presented in Ref. 43. Fig. (8) shows clearly the differences between the fractional fission gas release with and without grain growth process.

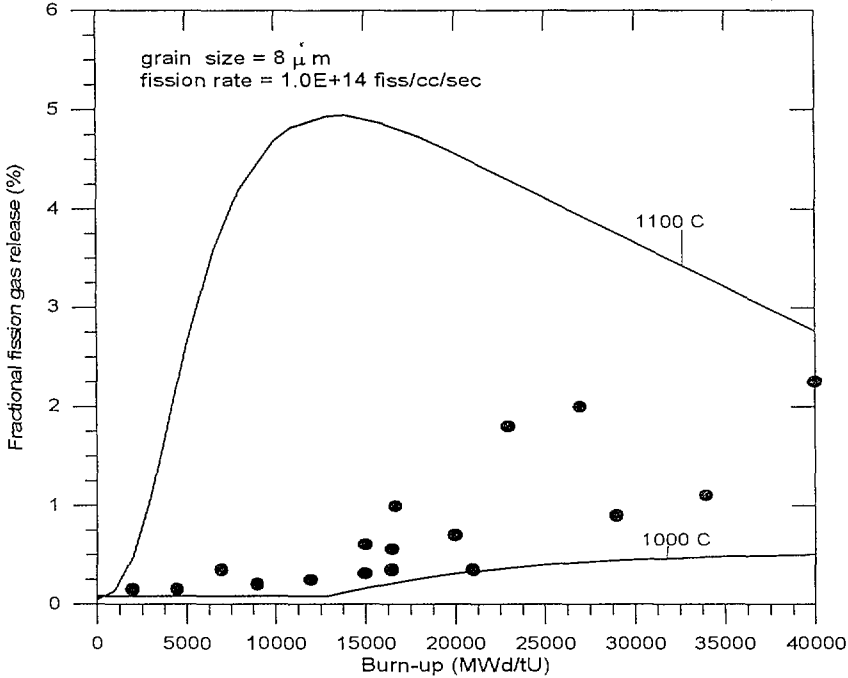


Fig. 7. Comparison of the fractional fission gas release as a function of burn-up with the experimental data copied from Fig. 2. of Ref. [44].

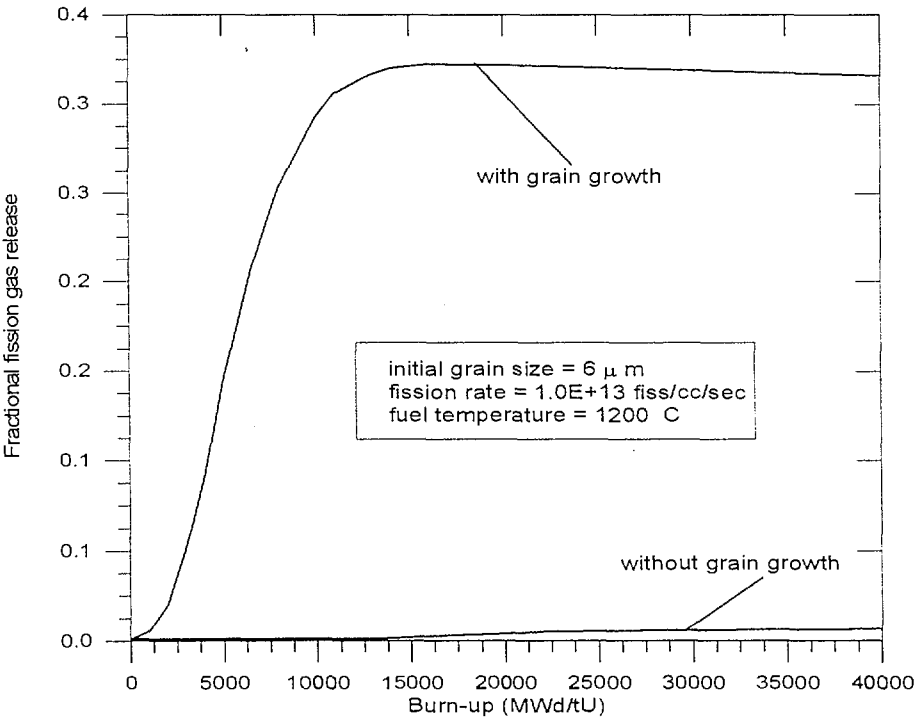


Fig. 8. Comparison between fractional fission gas release with and without grain growth.

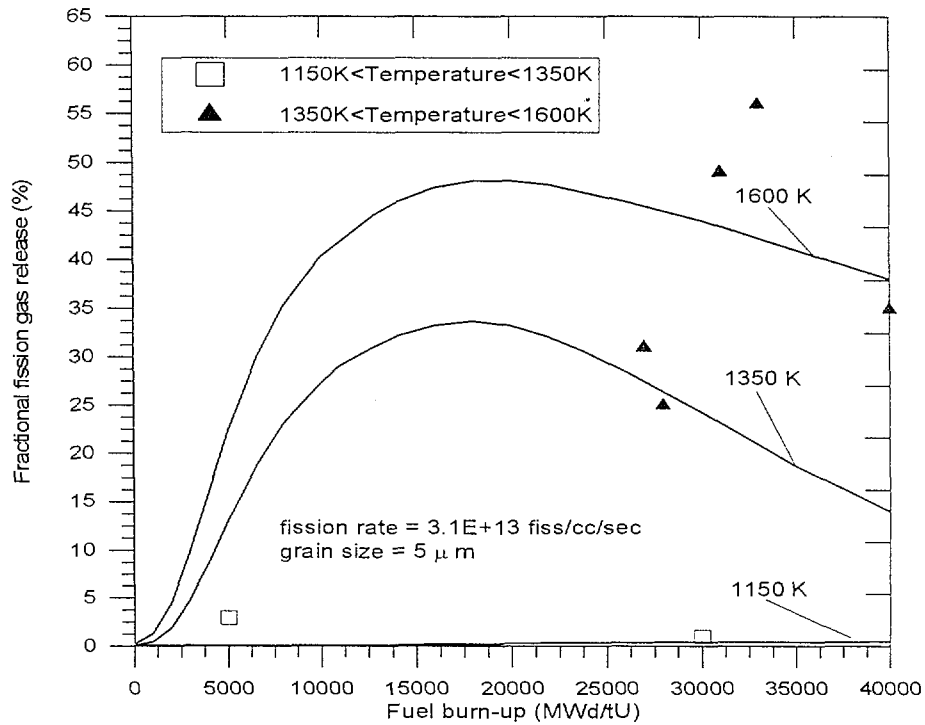


Fig. 9. Comparison of calculated fractional fission gas release as a function of burn-up with the experimental data copied from Fig. 3. of Ref. [37].

Fig. (9) shows the calculation of fractional fission gas release versus burnup for three temperatures (1150 , 1350 and 1600 K) which are compared with the experimental results presented in Ref. [36]. The experimental results are grouped for two temperature ranges 1150 – 1350 K and 1350 – 1600 K. Both Fig. (7) and Fig. (9) show a good agreement between the calculated and measured gas release, allowing for some scatter in the data.

8. CONCLUSIONS

The modification of grain growth equation is developed by taking under consideration two opposing effects of enhancement and inhibition of irradiation damage introduced by solid and gaseous fission products on grain growth rate. The behavior of fission gas within UO_2 fuel material is influenced by grain growth. The defect trap model of fission gas behaviour is improved by adding the grain growth process. The larger is the initial grain size the smaller is the fission gas release. The grain size is affected by the variation of the temperature and

burnup. The grain growth rate at temperature below 1300 K is negligible. At higher temperatures the grain growth is more pronounced. The calculated and experimental results are remarkably close, and therefore give us confidence in the completion of the model. In particular it supports the assumption that the Vitanza curve presents the recrystallization temperature of uranium dioxide grains.

References

- [1] F. Goldeanu, I. Furtuna and M. Paraschiu, *J. Nucl. Mater.* **148**, 351(1987).
- [2] Hj. Matzke, H. Blank, M. Coquerelle, C. Ronchi and C. T. Walker, *J. Nucl. Mater.* **166**, 165(1989).
- [3] KI-Seob Sim and Ho. Chun Suk, *Nucl. Technol.* **99**, 351(1992).
- [4] K. Une, K. Nogita and M. Imamura, *J. Nucl. Mater.* **188**, 65(1992).
- [5] J. E. Bainbridge, C. B. Forty and D. G. Martin, *J. Nucl. Mater.* **171**, 230(1990).
- [6] M. Hillert, *Acta Metallurgica*, **13**, 227 (1965).
- [7] W. D. Kingery and B. Francois, *J. Am. Ceram. Soc.*, **48**, 546 (196).
- [8] M.V. Speight and G.W. Greenwood, *Philosophical Magazine*, **9**, 683 (1964).
- [9] W.B. Lewis, J.R. MacEwan, W.H. Stevens, R.G. Hart, in: *Proc. of the 3 rd U.N. Conference on the peaceful Uses of Atomic Energy, Geneva, May 1964, p.*
- [10] J.A. Turnbull, *Radiation Effects Vol.* **53**, 243 (1980).
- [11] K. Shiba, *J. Nucl Mater.* **57**, 271(1975).
- [12] Y. Nogita, K. Une, *J. Nucl. Sci. Tech.* **30**, 900(1993).
- [13] K. Une, Sh. Kashibe, *J. Nucl. Sci. Tech.* **27(11)**2002(1990).
- [14] D.A. McInnes, P.W. Winter, *J. Phys. Chem. Solids Vol.* **49** 143(1988).
- [15] J. Leteutre and Y. Quere, *Irradiation Effects in Fissile Materials*, North Holland, Amstertam, 1972.
- [16] K. Lassman, C.T. Walker, J. Van de Laar, F. Lindstrom, *J. Nucl. Mater.* **26** 1(1995).
- [17] K. Nogita, K. Une, *Nucl. Inst. Met. In Phys. Reser.* **B 91** 301(1989).
- [18] C. Vitanza, E. Kolstad, Ü. Gracioni, *Proc. Of the American Nuclear Society, Topical Meeting on Light Water Reactors Fuel Performance*, Portland, Oregon, May 1979, p. 361.
- [19] C. S. Smith, *Trans. AIME.*, **175**, 15 (1948).
- [20] R. D. MacDonald, *J. Nucl. Mater.* **22**, 109(1972).
- [21] J.E. Burke, *Trans. Metall. Soc. AIME*, **180**, 73(1949).
- [22] I. Amoto, R. L. Colombo and A. M. Proti, *J. Am. Ceram. Soc.* **46**, 407(1963).
- [23] T. C. S. Hsieh, *Trans. Am. Nucl. Soc.* **27**, 377 (1977).
- [24] I. J. Hastings and J. A. Scoberg, *J. Nucl. Mater.* **82**, 435 (1979),
or AECL – 6411 (1979).
- [25] J. R. MacEwan, *J. Am. Ceram. Soc.* **45**, 37(1962).
- [26] J. R. MacEwan and J. Hayashi, *Proc. Brit. Ceram. Soc.* **7**, 245 (1967).
- [27] R. N. Singh, *J. Nucl. Mater.* **64**, 174 (1977).
- [28] M. F. Lyons, D. H. Choplin and B. Weidenbaum, *GEAP – 4411* (1963).
- [29] J. B. Ainscough, B. W. Oldfield and J. O. Ware, *J. Nucl. Mater.* **49** 117(1973/74).

- [30] C. Bagger, M. Mogensen, C.T. Walker, J. Nucl. Mater. **211** 11(1994).
- [31] M. Szuta, J. Nucl. Mater. **210** 178(1994).
- [32] H. Zimmermann, J. Nucl. Mater. **75** 154(1978).
- [33] R.J. White and M.O. Tucker, J. Nucl. Mater. **118** 1(1983).
- [34] T. Nakajima and H. Saito, Nucl. Eng. Des. **101** 267(1987).
- [35] K. Hiramoto, K. Miki, M. Nakamura, Nucl. Eng. Des. **81** 395(1984).
- [36] K. Ito, R. Iwasaki, Y. Iwano, J. Nucl. Sci. Techn. **22** 129(1985).
- [37] J. Rest, A.W. Cronenberg, J. Nucl. Mater. **150** 203(1987).
- [38] J.R. MacEwan, W.H. Stevens, J. Nucl. Mater. **11**, 1 77(1964).
- [39] I.L.F. Ray, H. Thiele, H.J. Matzke, J. Nucl. Mater. **58** 278(1975).
- [40] M. Szuta, J. Nucl. Mater. **58** 278(1975).
- [41] M. Szuta, J. Nucl. Mater. **97** 149(1981).
- [42] M. Szuta, J. Nucl. Mater. **130** 434(1985).
- [43] C.C. Dollins, J. Nucl. Mater. **49** 10(1973/74).